Glomerular permeability is not affected by heparan sulfate glycosaminoglycan deficiency in zebrafish embryos

Khalil, R.; Lalai, R.A.; Wiweger, M.I.; Avramut, C.M.; Koster, A.J.; Spaink, H.P.; ... ; Baelde, H.J.

Am J Physiol Renal Physiol 317: F1211–F1216, 2019.
First published August 28, 2019; doi:10.1152/ajprenal.00126.2019.

RESEARCH ARTICLE

Glomerular permeability is not affected by heparan sulfate glycosaminoglycan deficiency in zebrafish embryos

Ramzi Khalil,[1] Reshma A. Lalai,[1] Malgorzata I. Wiweger,[2] Cristina M. Avramut,[3] Abraham J. Koster,[3] Herman P. Spaink,[4] Jan A. Bruijn,[1] Pancras C. W. Hogendoorn,[1] and Hans J. Baelde[1]

[1]*Department of Pathology, Leiden University Medical Center, Leiden, The Netherlands;* [2]*International Institute of Molecular and Cell Biology in Warsaw, Warsaw, Poland;* [3]*Department of Cell and Chemical Biology, Leiden University Medical Center, Leiden, The Netherlands; and* [4]*Institute of Biology Leiden, Leiden University, Leiden, The Netherlands*

Submitted 12 March 2019; accepted in final form 25 August 2019

Khalil R, Lalai RA, Wiweger MI, Avramut CM, Koster AJ, Spaink HP, Bruijn JA, Hogendoorn PC, Baelde HJ. Glomerular permeability is not affected by heparan sulfate glycosaminoglycan deficiency in zebrafish embryos. *Am J Physiol Renal Physiol* 317: F1211–F1216, 2019. First published August 28, 2019; doi:10.1152/ajprenal.00126.2019.—Proteinuria develops when specific components in the glomerular filtration barrier have impaired function. Although the precise components involved in maintaining this barrier have not been fully identified, heparan sulfate proteoglycans are believed to play an essential role in maintaining glomerular filtration. Although in situ studies have shown that a loss of heparan sulfate glycosaminoglycans increases the permeability of the glomerular filtration barrier, recent studies using experimental models have shown that podocyte-specific deletion of heparan sulfate glycosaminoglycan assembly does not lead to proteinuria. However, tubular reabsorption of leaked proteins might have masked an increase in glomerular permeability in these models. Furthermore, not only podocytes but also glomerular endothelial cells are involved in heparan sulfate synthesis in the glomerular filtration barrier. Therefore, we investigated the effect of a global heparan sulfate glycosaminoglycan deficiency on glomerular permeability. We used a zebrafish embryo model carrying a homozygous germline mutation in the *ext2* gene. Glomerular permeability was assessed with a quantitative dextran tracer injection method. In this model, we accounted for tubular reabsorption. Loss of anionic sites in the glomerular basement membrane was measured using polyethyleneimine staining. Although mutant animals had significantly fewer negatively charged areas in the glomerular basement membrane, glomerular permeability was unaffected. Moreover, heparan sulfate glycosaminoglycan-deficient embryos had morphologically intact podocyte foot processes. Glomerular filtration remains fully functional despite a global reduction of heparan sulfate.

glomerular basement membrane; glomerular filtration barrier; heparan sulfate; proteinuria; zebrafish

INTRODUCTION

Proteinuria is associated with a wide variety of renal diseases. Proteinuria is an independent risk factor for loss of renal function, renal failure, and cardiovascular mortality (19, 25). Proteinuria occurs when proteins pass the glomerular filtration barrier (GFB) and are not fully reabsorbed by tubular epithelial cells; proteinuria can also develop when the reabsorption system is saturated. The GFB comprises fenestrated endothelial cells covered by a glycocalyx, the glomerular basement membrane (GBM), and podocyte foot processes (18). The GFB filters molecules based on size and charge (3).

The charge selectivity of the GFB has long been attributed primarily to heparan sulfate proteoglycans (HSPGs) in the GBM (21). HSPGs consist of a core protein to which heparan sulfate glycosaminoglycan (HS-GAG) chains are covalently attached. The HS-GAG chain is polymerized by enzymes encoded by the *EXT1* and *EXT2* genes. A defect in either is considered to be sufficient severely disrupt HS-GAG synthesis. Both during and after polymerization, the chain can be modified by several sulfotransferases and an epimerase, resulting in the addition of sulfate groups, which give HS-GAGs and thus the whole HSPG a negative net charge (8, 17).

HS-GAGs have been considered to be essential for GFB permeability as far back as 1980, when Kanwar et al. (20, 21) showed that enzymatic removal of HS-GAGs resulted in increased GBM permeability. These early results were supported by the finding that HSPG expression is reduced in several proteinuric renal diseases (34). However, recent findings in various mouse models have challenged the notion that HS-GAGs are essential for maintaining GFB permeability; these models include podocyte-specific knockouts of perlecan and agrin (two specific types of HSPGs) (10, 14), *Ext1* (4), *Extl3* (1), and *Ndst1* (an enzyme involved in GAG sulfation) (33). Although most of these models have a loss of anionic charge in the GBM, they do not develop significant proteinuria. However, HSPGs are also synthesized by mesangial cells and by glomerular endothelial cells (32, 35). HSPGs produced by glomerular endothelial cells have been shown to be important for GFB function, as removal of HS-GAG from glomerular endothelial cells results in increased permeability to albumin in in vitro experiments (32). The effects of an in vivo global HS-GAG deficiency on glomerular permeability remain unknown. Thus, the primary goal of the present study was to investigate the effect of a global (in contrast to a podocyte-specific) HS-GAG deficiency on glomerular permeability. In addition, although various experimental models using podocyte-specific HS-GAG deletion do not develop proteinuria, they may have increased glomerular permeability. Indeed, Chen et al. (4) hypothesized that a relatively moderate increase in tubular reabsorption may prevent proteinuria despite reduced glomerular permeability. To test this hypothesis, we

Address for reprint requests and other correspondence: R. Khalil, Dept. of Pathology, Leiden Univ. Medical Center, L1Q, Rm. P0-107, PO Box 9600, Leiden 2300 RC, The Netherlands (e-mail: R.Khalil@lumc.nl).

performed quantitative analyses using a zebrafish embryo model in which we could account for tubular reabsorption capacity.

MATERIALS AND METHODS

Animals. Zebrafish (*Danio rerio H*) embryos were collected from natural crosses and kept at 28.5°C in E3 medium. Wild-type (WT) AB/TL strain zebrafish embryos and *dackel* mutant (*dak/ext2*^{to273b}; referred to as "*dak/ext2*") zebrafish embryos were used for this study. Homozygous *dak/ext2* mutants contain a biallelic premature stop codon in the *ext2* gene. This mutation globally reduces zygotic *ext2* expression in homozygous *dak/ext2* mutants, resulting in impaired HS-GAG chain polymerization. Thus, HSPGs in homozygous mutants have truncated, functionally impaired HS-GAG side chains that are neither sulfated nor negatively charged (8). This model has been previously characterized with respect to HSPG distribution (5, 17, 23, 37). The total decrease of HS-GAGs in *dak/ext2* zebrafish embryos has previously been reported to be >80% (17, 23).

Homozygous *dak/ext2* mutants were sorted at 3 days postfertilization (dpf) based on cranofacial, ear, and fin phenotypes as previously described (36, 38). Embryos from separate crosses were used for each experiment.

All experiments were performed on embryos before the free feeding stage and therefore did not fall under the animal experimentation law in accordance with to European Union Animal Protection Directive 2010/63/EU.

Electron microscopy. WT and homozygous *dak/ext2* embryos at 3 and 5 dpf were anesthetized with 4% tricaine methanesulfonate (4 mg/ml), chemically fixed for 1 h in 1.5% glutaraldehyde in 0.1 M sodium cacodylate buffer (pH 7.4), rinsed twice with 0.1 M sodium cacodylate, incubated for 1 h in 1% osmium tetroxide in 0.1 M sodium cacodylate buffer, dehydrated sequentially in 70%, 80%, 90%, and 100% ethanol, and then immersed in 1:1 propylene oxide-epon LX-112 solution for 1 h. The fish were then washed, infiltrated with pure epon for 2 h, embedded in epon LX-112, and polymerized at 60°C for 2 days.

Ultrathin sections (100 nm) were mounted on copper slot grids (Storck Veco, Eerbeek, The Netherlands), covered with formvar film and carbon layer, and then stained with an aqueous solution of 7% uranyl acetate for 20 min followed by Reynold's lead citrate for 10 min. Specimens were imaged at an acceleration voltage of 120 kV using a Tecnai 12 BioTWIN transmission electron microscope (FEI, Eindhoven, The Netherlands), equipped with a FEI 4k Eagle CCD camera. Virtual slides of zebrafish glomeruli were recorded at ×18,500 magnification, corresponding to a 1.2-nm pixel size at the specimen level, using automated data acquisition and stitching software (9).

Loss of anionic sites in the GBM. The number of anionic sites in the GBM was measured using polyethylenimine (PEI) staining, as previously described (6, 16). Specifically, we measured the number of PEI particles per micrometer of GBM. PEI is a cationic polymer that binds to anionic sites. It was used as a surrogate marker for HS-GAG, as HS-GAG are highly sulfated and therefore negatively charged. PEI is not specific to HS-GAG, as it binds to all anionic sites. Two samples each of homozygous *dak/ext2* and WT embryos were incubated in 1% PEI (PEI-600, Polysciences, Warrington, PA) in 0.1 M sodium cacodylate buffer (pH 7.4) for 6 h with constant agitation. Samples were washed after incubation and subsequently fixed with 2% phosphotungstic acid and 1% glutaraldehyde. Samples were then stained with 1% osmium tetroxide and embedded in epon LX-112. A selection of representative images containing at least 13 μm of GBM was analyzed using transmission electron microscopy.

Foot process width. Foot process width was analyzed using a selection of representative electron microscopy images obtained from three different homozygous *dak/ext2* mutants and three different WT embryos. All images contained at least 9 μm of contiguous GBM. The following formula: $\frac{\pi}{4}\times\frac{\sum \text{GBM length}}{\sum \text{Foot processes}}$ was used to calculate foot process width (11).

Assessing glomerular permeability. The quantitative dextran tracer injection method [adapted from the qualitative method previously described by Ebarasi et al. (7)] was used to measure glomerular permeability. This method is not used for an assessment of charge or size selectivity but for analyzing functionally significant alterations to the global permeability of the GFB. A total of 32 homozygous *dak/ext2* and 35 WT embryos were used for 4 experiments as follows: at 5 dpf, zebrafish embryos were anesthetized with 4% tricaine methanesulfonate (4 mg/ml) injected intravenously with 1 nl of a mixture containing FITC-labeled lysine-fixable 70-kDa dextran (25 mg/ml, Invitrogen, Waltham, MA) and TRITC-labeled 3-kDa dextran (100 mg/ml, Invitrogen). As a positive control, WT zebrafish embryos were also injected with puromycin aminonucleoside (PAN; Sigma-Aldrich, St. Louis, MO) at 4 dpf (15). One hour after dextrans were injected, samples were fixed in 10% formalin for 24 h and stored in 70% ethanol until further processing. Samples were then embedded in paraffin, sectioned at 4 μm thickness, and examined using immunofluorescence microscopy. Samples were analyzed in a blinded manner.

Under physiological conditions, 3-kDa dextran can readily pass the GFB, whereas 70-kDa dextran does not. If the integrity of the GFB is sufficiently compromised, the 70-kDa dextran can pass the GFB, after which it is reabsorbed by proximal tubule epithelial cells in endosomes. Therefore, we measured the number of 70-kDa dextran particles in proximal tubule cells as a measure of glomerular permeability. To confirm functional tubular reabsorption, we also measured the number of 3-kDa dextran particles in proximal tubule cells.

Statistical analyses. Statistical analyses were performed using SPSS (version 20.0, IBM, Armonk, NY). The proportion of zebrafish embryos with pericardial edema was analyzed using Fisher's exact test. Dextran tracer measurements of glomerular permeability, foot process width, and the presence of anionic sites were analyzed using a Student's unpaired *t*-test. Differences with $P < 0.05$ were considered significant.

RESULTS

The dackel mutant phenotype. Homozygous *dak/ext2*^{to273b} (referred to hereafter as simply "*dak/ext2*") mutants develop a clear phenotype, as previously described (15). Consistent with previous reports, compared with WT embryos, mutant embryos lacked pectoral fins and had a protruding jaw, a noninflated swim bladder, and a more concave body shape (6, 36). In addition, homozygous *dak/ext2* mutants had a significantly higher prevalence of pericardial edema compared with WT embryos (31/34 vs. 1/140 embryos, respectively, $P < 0.0001$). An example of morphological changes and pericardial edema in a mutant embryo is shown in Fig. 1.

Loss of anionic sites in the GBM. Because HS-GAGs are believed to be the primary contributor to the negative charge in the GBM (20), we expected that the loss of HS-GAGs in homozygous *dak/ext2* mutants would result in reduced numbers of negatively charged sites in the GBM. We therefore tested this hypothesis using PEI staining (31); PEI molecules bind to negatively charged sites and form electron-dense deposits. Consistent with our hypothesis, the mean number of electron-dense deposits per micrometers of GBM was significantly lower in homozygous *dak/ext2* mutants compared with WT embryos [0.80 (SD 0.39), $n = 2$, vs. 2.2 (SD 0.72), $n = 2$, respectively, $P < 0.05$; Fig. 2].

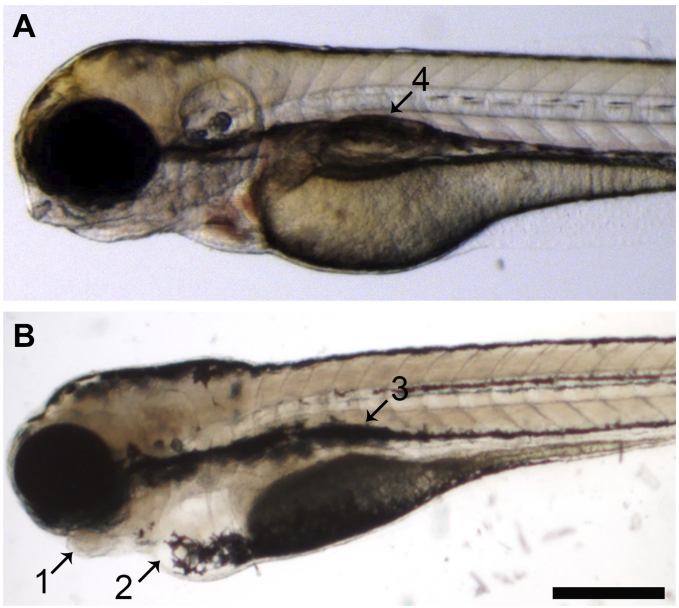

Fig. 1. Homozygous *dak/ext2* mutant zebrafish develop morphological changes. *A* and *B*: examples of a wild-type (WT; *A*) embryo and a homozygous *dak/ext2* (*B*) embryo at 5 days postfertilization, with several morphological changes in the mutant embryos. *Arrows 1*, *2*, and *3* indicate a protruding jaw, pericardial edema, and a noninflated swim bladder, respectively; *arrow 4* shows a normally developed swim bladder in the WT embryo. Scale bar = 250 μm.

Foot process width. Ultrastructural analysis of the GFB using transmission electron microscopy revealed normal foot processes (Fig. 2) in homozygous *dak/ext2* mutants. The mean width of foot process did not differ significantly between homozygous *dak/ext2* mutants and WT embryos [0.181 (SD 0.025), $n = 3$, vs. 0.176 (SD 0.012), $n = 3$, $P = 0.76$].

Glomerular permeability. Next, we analyzed the reabsorption of injected dextran particles (Fig. 3). We found no significant difference between homozygous *dak/ext2* mutants and WT embryos with respect to the mean number of reabsorbed 3-kDa dextran droplets [22.69 (SD 10.22), $n = 32$, vs. 24.33 (SD 12.51), $n = 21$, $P = 0.60$). PAN-injected WT embryos, which were used as a positive control, had a similar number of 3-kDa dextran droplets [25.79 (SD 13.33), $n = 14$, $P = 0.75$ vs. WT and $P = 0.39$ vs. homozygous *dak/ext2*). As small particles can pass readily through the GFB, the similar number of 3-kDa dextran droplets indicates fully functional tubular reabsorption in all groups.

We also found no significant difference between homozygous *dak/ext2* mutants and WT embryos with respect to 70-kDa dextran particles. The mean number of droplets WT PAN-injected embryos had significantly more 70-kDa droplets [16.93 (SD 5.41), $n = 14$] compared with both WT embryos ($P < 0.0001$) and *dak/ext2* mutants ($P < 0.0001$). Taken together, these data indicate that 70-kDa particles pass the GFB in similar quantities under physiological conditions and in a HS-GAG-free environment.

DISCUSSION

Here, we investigated whether HS-GAGs play an essential role in glomerular permeability using homozygous *dak/ext2* mutant zebrafish in which HS-GAGs are lacking in the entire embryo. We found that homozygous *dak/ext2* mutants develop an overall phenotype similar to previous reports (6, 36). PEI staining of the GBM revealed significantly fewer anionic sites in homozygous mutants compared with WT embryos; however, despite having fewer negative sites in the GBM, homozygous *dak/ext2* mutants had normal glomerular permeability. Furthermore, our ultrastructural analysis revealed no difference between homozygous *dak/ext2* mutants and WT embryos with respect to podocyte foot width.

The classic paradigm based on the results of Kanwar et al. (21, 29) suggests that HS-GAGs are essential for normal glomerular filtration. In their study, the authors found that

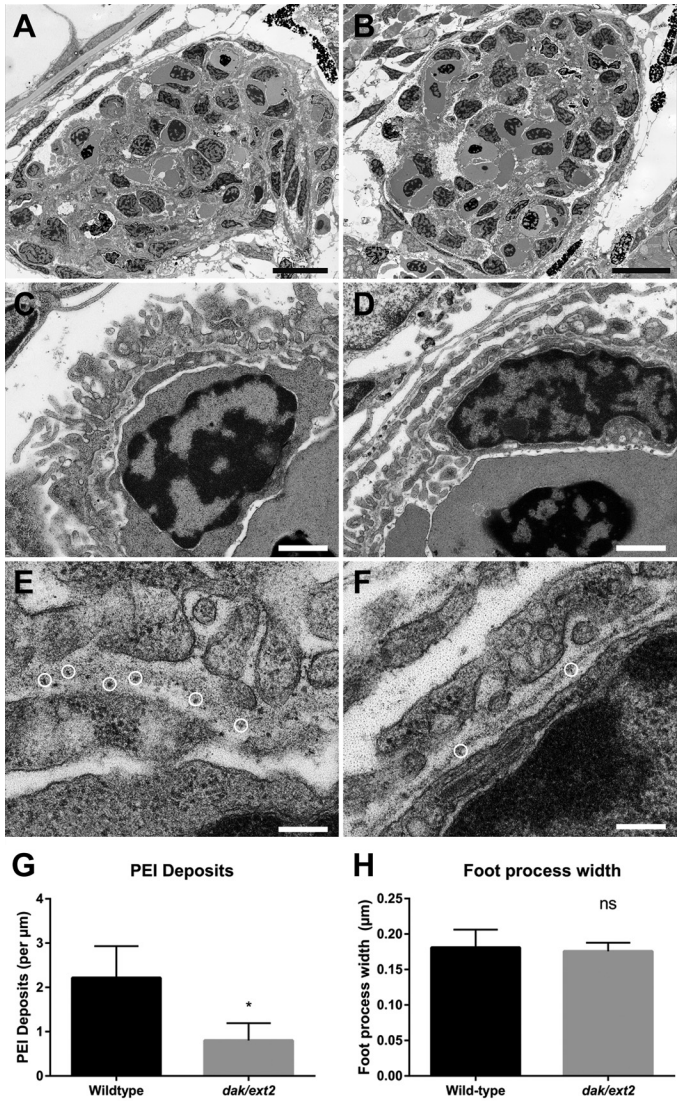

Fig. 2. Homozygous *dak/ext2* mutant zebrafish have significantly fewer electron dense-deposits in the glomerular basement membrane (GBM) but normal podocyte foot process width. *A–F*: transmission electron micrographs of the glomerulus (*A* and *B*), a capillary loop (*C* and *D*), and representative sections of GBM (*E* and *F*) in a wild-type (*A*, *C*, and *E*) and homozygous *dak/ext2* mutant (*B*, *D*, and *F*) embryo. Sections were stained with polyethylenimine (PEI) particles, which bind to negatively charged molecules in the GBM, forming electron-dense deposits (examples indicated by white circles in *E* and *F*). *G*: summary of the number of electron-dense PEI-containing deposits in the GBM. $*P < 0.05$. *H*: summary of the foot process width. ns, not significant ($P > 0.05$). Scale bars = 10 μm in *A* and *B*, 1 μm in *C* and *D*, and 200 nm in *E* and *F*.

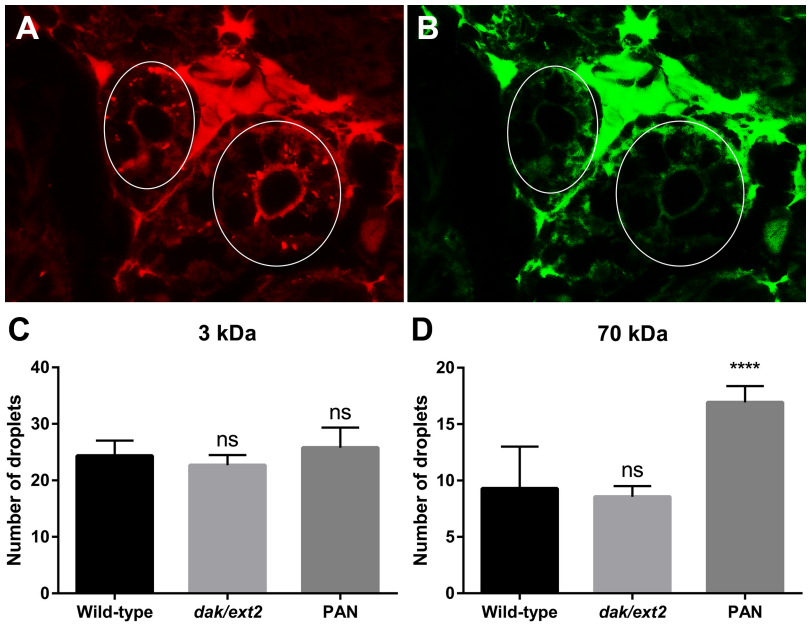

Fig. 3. Homozygous *dak/ext2* mutant zebrafish have normal glomerular permeability and tubular reabsorption capacity. *A* and *B*: transverse sections through the proximal tubular epithelium of homozygous *dak/ext2* mutant embryos injected with red fluorescent 3-kDa dextran (*A*) and green fluorescent 70-kDa dextran (*B*). The white ellipse highlights proximal tubule epithelial cells. The bright area between the circle reflects background fluorescence, partly due to autofluorescence. *C* and *D*: summary of the number of 3-kDa (*C*) and 70-kDa (*D*) dextran droplets in wild-type, homozygous *dak/ext2* mutant, and puromycin aminonucleoside (PAN)-injected wild-type embryos. ns, not significant ($P > 0.05$ vs. wild type). ****$P < 0.0001$ vs. wild type. A digital high-pass filter was placed over *A* and *B* to enhance the contrast between reabsorption droplets and the surrounding tissue. Scale bar = 5 μm.

glomerular permeability increased after perfusing the kidney with heparinase III, an enzyme that cleaves HS-GAG chains. However, several other studies have shown that podocyte-specific knockout of HS-GAGs did not result in proteinuria, suggesting that HS-GAGs may not necessarily be required for normal glomerular filtration (1, 4, 10, 14, 33). Consistent with this notion, our results show that even when HS-GAGs are deleted in the entire embryo (and not specifically in podocytes), glomerular filtration is essentially intact. It remains possible that the size- and charge-selective properties of the GFB are altered in HS-GAG deficiency. However, overall glomerular permeability remains intact despite a severe and global loss of HS-GAG, as was hypothesized.

Previous in vivo models of HS-GAG deficiency used proteinuria as a readout of glomerular permeability; thus, albumin retrieval by proximal tubule epithelial cells may have masked changes in glomerular permeability, as suggested by Chen et al. (4). Therefore, we used tubular reabsorption of 70-kDa dextran particles as our readout of glomerular permeability; this method has been previously reported as providing a reliable measure of overall glomerular permeability (13, 15). Although dextrans are known to move through a network as chains rather than as hydrodynamic spheres, dextrans have been validated as a sensitive marker for loss of glomerular permeability in various zebrafish models (12, 13, 15, 22, 28). Tubular reabsorption mechanisms were found to be fully functional in homozygous *dak/ext2* mutants, as a similar number of 3-kDa dextran droplets, which readily pass the GFB, were found between mutant and wild-type embryos.

Pericardial edema has been previously used as an indicator of renal damage in zebrafish (13). Interestingly, although homozygous *dak/ext2* mutants lack HS-GAGs throughout the entire body and develop pericardial edema, they have essentially normal glomerular permeability. We therefore speculate that the pericardial edema observed in homozygous *dak/ext2* mutants is not caused by renal damage. For example, HS-GAG deficiency may have had an effect on the permeability of systemic capillaries because of an altered glycocalyx composition. Such a correlation between the endothelial glycocalyx of systemic capillaries and vascular permeability has been previously reported (30).

An important difference between the study by Kanwar et al. (21, 29) and our approach using a germline mutation is that Kanwar et al. investigated the acute loss of HS-GAG by enzymatic activity, whereas our approach deleted HS-GAGs for an extended period. This difference may account for the difference in results between the two studies. For example, with a germline mutation, the effects will be present throughout the animal's life; therefore, other GAGs may have functionally replaced the deleted HS-GAGs. In the in situ setup used by Kanwar et al., loss of HS-GAG is acute and there is not enough time for such a compensatory mechanism to take place. Another possible explanation for the different results is that the enzymes used by Kanwar et al. may have caused collateral damage to other components of the GFB, which could have led to their observed increase in glomerular permeability.

The charge-selective nature of the GBM has long been attributed to the presence of HS-GAG (20). In contrast, Miner (26) proposed that charge selectivity is not an essential factor in glomerular permeability, as several studies found that a decreased number of anionic sites does not necessarily coincide with proteinuria. Consistent with this notion, we found that glomerular permeability was not affected in homozygous *dak/ext2* mutants, despite the fact that these animals had significantly fewer PEI particles in the GBM. It is important to note that although negatively charged sites were significantly reduced in the GBM of homozygous *dak/ext2* mutants, these sites were not completely absent. Thus, these residual anionic sites could reflect negatively charged particles other than HS-GAGs. For example, collagen type IV, which is one of the primary constituents of the GBM, contains negatively charged sialic acid residues (27). Therefore, we cannot exclude the possibility that the residual negatively charged sites in the GBM are sufficient for conferring charge selectivity.

Our ultrastructural analysis of the glomeruli in zebrafish embryos revealed that homozygous *dak/ext2* mutants have

normal podocyte foot processes. Although similar results were reported in podocyte-specific agrin-deficient and perlecan-deficient mice, podocyte-specific *Ext1* knockout mice have foot process effacement (4, 10, 14). The difference between our global *ext2*-deficient zebrafish model and podocyte-specific *Ext1* knockout mice may be due to differential effects of Ext1 and Ext2 on podocyte cytoskeletal organization. Both EXT1 and EXT2 have been reported to influence cytoskeletal organization in chondrocytes obtained from patients with EXT1 or EXT2 mutations (2), in which the specific mutation seemed to determine the effect on cytoskeletal organization. Whether EXT1 and/or EXT2 directly affects cytoskeletal organization in podocytes, independently of HS-GAG side chains, remains an open question.

This study has several limitations. First, a direct local decrease in HS-GAGs could not be shown by immunohistochemistry. However, *dak/ext2* mutants had significantly less anionic sites in the GBM than WT animals in our PEI labeling experiment. This is indirect proof of a decrease in HS-GAGs. Thus, the degree of HS-GAG deficiency in the glomerulus is at least 63%, as this is the relative difference in PEI particles. These particles could reflect HS-GAGs, other sulfated GAGs, or other negatively charged areas. Also, the total decrease of HS-GAGs in *dak/ext2* zebrafish embryos has previously been reported to be >80% (17, 23). Although a relative and significant decrease in PEI-particles was observed, the absolute extent of PEI labeling is less than in mammalian systems. A possible explanation is that this is due to a methodological difference, as we did not perform an in vivo labeling (4). Also, it could be a reflection of interspecies variation in anionic site distribution in the GBM.

Furthermore, the *dak/ext2* model does not have a complete loss of HS-GAG. Theoretically, a double knockout of ext1 and ext2 would result in even more pronounced loss of HS-GAG. As zebrafish have three ext1 genes (ext1a, ext1b, and ext1c) and up to date characterized mutants lines are not available for any of these semiorthologs, this could not be confirmed experimentally. To the best of our knowledge, this is the first study to examine the effect of a global HS-GAG deficiency on glomerular permeability. Globally deleting HS-GAGs in most vertebrates causes extremely early lethality (24); Thus the homozygous *dak/ext2* mutant zebrafish is currently the only viable model for global loss of HS-GAGs that survives gastrulation when both copies of the ext2 gene are impaired and that gives unique opportunity to study glomerular filtration that cannot be rescued by HS-GAGs produced by other type of cells. Although homozygous *dak/ext2* mutants do not survive to adulthood, Lee et al. (23) hypothesized that these mutants survive the first part of the embryonic phase due to the maternal contribution of Ext2; by 5 dpf, maternal contribution of Ext2 decreases to nondetectable levels.

In conclusion, we provide the first report showing that glomerular permeability is not affected by global HS-GAG deficiency. These results support the growing body of evidence that HS-GAGs do not play an essential role in mediating glomerular permeability.

ACKNOWLEDGMENTS

We thank Peter Neeskens and Brendy van den Akker for assistance with electron microscopy experiments.

GRANTS

This work was supported by Dutch National Kidney Foundation Grant IP 11.57.

DISCLOSURES

No conflicts of interest, financial or otherwise, are declared by the authors.

AUTHOR CONTRIBUTIONS

R.K., M.I.W., C.M.A., A.J.K., H.P.S., J.A.B., P.C.H., and H.J.B. conceived and designed research; R.K., R.A.L., M.I.W., and C.M.A. performed experiments; R.K. and R.A.L. analyzed data; R.K., M.I.W., C.M.A., H.P.S., J.A.B., P.C.H., and H.J.B. interpreted results of experiments; R.K. prepared figures; R.K. drafted manuscript; R.K., M.I.W., C.M.A., P.C.H., and H.J.B. edited and revised manuscript; R.K., R.A.L., M.I.W., C.M.A., A.J.K., H.P.S., J.A.B., P.C.H., and H.J.B. approved final version of manuscript.

REFERENCES

1. **Aoki S, Saito-Hakoda A, Yoshikawa T, Shimizu K, Kisu K, Suzuki S, Takagi K, Mizumoto S, Yamada S, van Kuppevelt TH, Yokoyama A, Matsusaka T, Sato H, Ito S, Sugawara A.** The reduction of heparan sulphate in the glomerular basement membrane does not augment urinary albumin excretion. *Nephrol Dial Transplant* 33: 26–33, 2018. doi:10.1093/ndt/gfx218.
2. **Bernard MA, Hogue DA, Cole WG, Sanford T, Snuggs MB, Montufar-Solis D, Duke PJ, Carson DD, Scott A, Van Winkle WB, Hecht JT.** Cytoskeletal abnormalities in chondrocytes with EXT1 and EXT2 mutations. *J Bone Miner Res* 15: 442–450, 2000. doi:10.1359/jbmr.2000.15.3.442.
3. **Brenner BM, Hostetter TH, Humes HD.** Molecular basis of proteinuria of glomerular origin. *N Engl J Med* 298: 826–833, 1978. doi:10.1056/NEJM197804132981507.
4. **Chen S, Wassenhove-McCarthy DJ, Yamaguchi Y, Holzman LB, van Kuppevelt TH, Jenniskens GJ, Wijnhoven TJ, Woods AC, McCarthy KJ.** Loss of heparan sulfate glycosaminoglycan assembly in podocytes does not lead to proteinuria. *Kidney Int* 74: 289–299, 2008. doi:10.1038/ki.2008.159.
5. **Clément A, Wiweger M, von der Hardt S, Rusch MA, Selleck SB, Chien CB, Roehl HH.** Regulation of zebrafish skeletogenesis by ext2/dackel and papst1/pinscher. *PLoS Genet* 4: e1000136, 2008. doi:10.1371/journal.pgen.1000136.
6. **de Andrea CE, Prins FA, Wiweger MI, Hogendoorn PC.** Growth plate regulation and osteochondroma formation: insights from tracing proteoglycans in zebrafish models and human cartilage. *J Pathol* 224: 160–168, 2011. doi:10.1002/path.2886.
7. **Ebarasi L, He L, Hultenby K, Takemoto M, Betsholtz C, Tryggvason K, Majumdar A.** A reverse genetic screen in the zebrafish identifies crb2b as a regulator of the glomerular filtration barrier. *Dev Biol* 334: 1–9, 2009. doi:10.1016/j.ydbio.2009.04.017.
8. **Esko JD, Selleck SB.** Order out of chaos: assembly of ligand binding sites in heparan sulfate. *Annu Rev Biochem* 71: 435–471, 2002. doi:10.1146/annurev.biochem.71.110601.135458.
9. **Faas FG, Avramut MC, van den Berg BM, Mommaas AM, Koster AJ, Ravelli RB.** Virtual nanoscopy: generation of ultra-large high resolution electron microscopy maps. *J Cell Biol* 198: 457–469, 2012. doi:10.1083/jcb.201201140.
10. **Goldberg S, Harvey SJ, Cunningham J, Tryggvason K, Miner JH.** Glomerular filtration is normal in the absence of both agrin and perlecan-heparan sulfate from the glomerular basement membrane. *Nephrol Dial Transplant* 24: 2044–2051, 2009. doi:10.1093/ndt/gfn758.
11. **Gundersen HJ, Seefeldt T, Osterby R.** Glomerular epithelial foot processes in normal man and rats. Distribution of true width and its intra- and inter-individual variation. *Cell Tissue Res* 205: 147–155, 1980. doi:10.1007/BF00234450.
12. **Hanke N, King BL, Vaske B, Haller H, Schiffer M.** A fluorescence-based assay for proteinuria screening in larval zebrafish (*Danio rerio*). *Zebrafish* 12: 372–376, 2015. doi:10.1089/zeb.2015.1093.
13. **Hanke N, Staggs L, Schroder P, Litteral J, Fleig S, Kaufeld J, Pauli C, Haller H, Schiffer M.** "Zebrafishing" for novel genes relevant to the glomerular filtration barrier. *BioMed Res Int* 2013: 658270, 2013. doi:10.1155/2013/658270.
14. **Harvey SJ, Jarad G, Cunningham J, Rops AL, van der Vlag J, Berden JH, Moeller MJ, Holzman LB, Burgess RW, Miner JH.** Disruption of

glomerular basement membrane charge through podocyte-specific mutation of agrin does not alter glomerular permselectivity. *Am J Pathol* 171: 139–152, 2007. doi:10.2353/ajpath.2007.061116.

15. **Hentschel DM, Mengel M, Boehme L, Liebsch F, Albertin C, Bonventre JV, Haller H, Schiffer M.** Rapid screening of glomerular slit diaphragm integrity in larval zebrafish. *Am J Physiol Renal Physiol* 293: F1746–F1750, 2007. doi:10.1152/ajprenal.00009.2007.
16. **Hogendoorn PC, de Heer E, Weening JJ, Daha MR, Hoedemaeker PJ, Fleuren GJ.** Glomerular capillary wall charge and antibody binding in passive Heymann nephritis. *J Lab Clin Med* 111: 150–157, 1988.
17. **Holmborn K, Habicher J, Kasza Z, Eriksson AS, Filipek-Gorniok B, Gopal S, Couchman JR, Ahlberg PE, Wiweger M, Spillmann D, Kreuger J, Ledin J.** On the roles and regulation of chondroitin sulfate and heparan sulfate in zebrafish pharyngeal cartilage morphogenesis. *J Biol Chem* 287: 33905–33916, 2012. doi:10.1074/jbc.M112.401646.
18. **Jeansson M, Haraldsson B.** Morphological and functional evidence for an important role of the endothelial cell glycocalyx in the glomerular barrier. *Am J Physiol Renal Physiol* 290: F111–F116, 2006. doi:10.1152/ajprenal.00173.2005.
19. **Jungers P, Hannedouche T, Itakura Y, Albouze G, Descamps-Latscha B, Man NK.** Progression rate to end-stage renal failure in non-diabetic kidney diseases: a multivariate analysis of determinant factors. *Nephrol Dial Transplant* 10: 1353–1360, 1995.
20. **Kanwar YS, Farquhar MG.** Presence of heparan sulfate in the glomerular basement membrane. *Proc Natl Acad Sci USA* 76: 1303–1307, 1979. doi:10.1073/pnas.76.3.1303.
21. **Kanwar YS, Linker A, Farquhar MG.** Increased permeability of the glomerular basement membrane to ferritin after removal of glycosaminoglycans (heparan sulfate) by enzyme digestion. *J Cell Biol* 86: 688–693, 1980. doi:10.1083/jcb.86.2.688.
22. **Laurent TC, Sundelöf LO, Wik KO, Wärmegård B.** Diffusion of dextran in concentrated solutions. *Eur J Biochem* 68: 95–102, 1976. doi:10.1111/j.1432-1033.1976.tb10767.x.
23. **Lee JS, von der Hardt S, Rusch MA, Stringer SE, Stickney HL, Talbot WS, Geisler R, Nüsslein-Volhard C, Selleck SB, Chien CB, Roehl H.** Axon sorting in the optic tract requires HSPG synthesis by ext2 (dackel) and extl3 (boxer). *Neuron* 44: 947–960, 2004. doi:10.1016/j.neuron.2004.11.029.
24. **Lin X, Wei G, Shi Z, Dryer L, Esko JD, Wells DE, Matzuk MM.** Disruption of gastrulation and heparan sulfate biosynthesis in EXT1-deficient mice. *Dev Biol* 224: 299–311, 2000. doi:10.1006/dbio.2000.9798.
25. **Matsushita K, van der Velde M, Astor BC, Woodward M, Levey AS, de Jong PE, Coresh J, Gansevoort RT; Chronic Kidney Disease Prognosis Consortium.** Association of estimated glomerular filtration rate and albuminuria with all-cause and cardiovascular mortality in general population cohorts: a collaborative meta-analysis. *Lancet* 375: 2073–2081, 2010. doi:10.1016/S0140-6736(10)60674-5.
26. **Miner JH.** Glomerular filtration: the charge debate charges ahead. *Kidney Int* 74: 259–261, 2008. doi:10.1038/ki.2008.260.
27. **Nayak BR, Spiro RG.** Localization and structure of the asparagine-linked oligosaccharides of type IV collagen from glomerular basement membrane and lens capsule. *J Biol Chem* 266: 13978–13987, 1991.
28. **Rider SA, Bruton FA, Collins RG, Conway BR, Mullins JJ.** The efficacy of puromycin and adriamycin for induction of glomerular failure in larval zebrafish validated by an assay of glomerular permeability dynamics. *Zebrafish* 15: 234–242, 2018. doi:10.1089/zeb.2017.1527.
29. **Rosenzweig LJ, Kanwar YS.** Removal of sulfated (heparan sulfate) or nonsulfated (hyaluronic acid) glycosaminoglycans results in increased permeability of the glomerular basement membrane to 125I-bovine serum albumin. *Lab Invest* 47: 177–184, 1982.
30. **Salmon AH, Satchell SC.** Endothelial glycocalyx dysfunction in disease: albuminuria and increased microvascular permeability. *J Pathol* 226: 562–574, 2012. doi:10.1002/path.3964.
31. **Schurer JW, Hoedemaeker J, Molenaar I.** Polyethyleneimine as tracer particle for (immuno) electron microscopy. *J Histochem Cytochem* 25: 384–387, 1977. doi:10.1177/25.5.325123.
32. **Singh A, Satchell SC, Neal CR, McKenzie EA, Tooke JE, Mathieson PW.** Glomerular endothelial glycocalyx constitutes a barrier to protein permeability. *J Am Soc Nephrol* 18: 2885–2893, 2007. doi:10.1681/ASN.2007010119.
33. **Sugar T, Wassenhove-McCarthy DJ, Esko JD, van Kuppevelt TH, Holzman L, McCarthy KJ.** Podocyte-specific deletion of NDST1, a key enzyme in the sulfation of heparan sulfate glycosaminoglycans, leads to abnormalities in podocyte organization in vivo. *Kidney Int* 85: 307–318, 2014. doi:10.1038/ki.2013.281.
34. **van den Born J, van den Heuvel LP, Bakker MA, Veerkamp JH, Assmann KJ, Weening JJ, Berden JH.** Distribution of GBM heparan sulfate proteoglycan core protein and side chains in human glomerular diseases. *Kidney Int* 43: 454–463, 1993. doi:10.1038/ki.1993.67.
35. **van Det NF, van den Born J, Tamsma JT, Verhagen NA, Berden JH, Bruijn JA, Daha MR, van der Woude FJ.** Effects of high glucose on the production of heparan sulfate proteoglycan by mesangial and epithelial cells. *Kidney Int* 49: 1079–1089, 1996. doi:10.1038/ki.1996.157.
36. **van Eeden FJ, Granato M, Schach U, Brand M, Furutani-Seiki M, Haffter P, Hammerschmidt M, Heisenberg CP, Jiang YJ, Kane DA, Kelsh RN, Mullins MC, Odenthal J, Warga RM, Nüsslein-Volhard C.** Genetic analysis of fin formation in the zebrafish, Danio rerio. *Development* 123: 255–262, 1996.
37. **Wiweger MI, Avramut CM, de Andrea CE, Prins FA, Koster AJ, Ravelli RB, Hogendoorn PC.** Cartilage ultrastructure in proteoglycan-deficient zebrafish mutants brings to light new candidate genes for human skeletal disorders. *J Pathol* 223: 531–542, 2011. doi:10.1002/path.2824.
38. **Wiweger MI, Zhao Z, van Merkesteyn RJ, Roehl HH, Hogendoorn PC.** HSPG-deficient zebrafish uncovers dental aspect of multiple osteochondromas. *PLoS One* 7: e29734, 2012. doi:10.1371/journal.pone.0029734.